

Rapid desensitization of the nitric oxide receptor, soluble guanylyl cyclase, underlies diversity of cellular cGMP responses

Tomas C. Bellamy*, John Wood^{†‡}, David A. Goodwin*, and John Garthwaite*[§]

*The Wolfson Institute for Biomedical Research, University College London, Gower Street, London WC1E 6BT, United Kingdom; and [†]Department of Health Sciences, University of York, York YO1 5DD, United Kingdom

Communicated by Michael J. Berridge, The Babraham Institute, Cambridge, United Kingdom, December 31, 1999 (received for review November 21, 1999)

A major receptor for nitric oxide (NO) is the cGMP-synthesizing enzyme, soluble guanylyl cyclase (sGC), but it is not known how this enzyme behaves in cells. In cerebellar cells, NO (from diethylamine NONOate) increased astrocytic cGMP with a potency ($EC_{50} \leq 20$ nM) higher than that reported for purified sGC. Deactivation of NO-stimulated sGC activity, studied by trapping free NO with hemoglobin, took place within seconds (or less) rather than the minute time scale reported for the purified enzyme. Measurement of the rates of accumulation and degradation of cGMP were used to follow the activity of sGC over time. The peak activity, occurring within seconds of adding NO, was swiftly followed by desensitization to a steady-state level 8-fold lower. The same desensitizing profile was observed when the net sGC activity was increased or decreased or when cGMP breakdown was inhibited. Recovery from desensitization was relatively slow (half-time = 1.5 min). When the cells were lysed, sGC desensitization was lost. Analysis of the transient cGMP response to NO in human platelets showed that sGC underwent a similar desensitization. The results indicate that, in its natural environment, sGC behaves much more like a neurotransmitter receptor than had been expected from previous enzymological studies, and that hitherto unknown sGC regulatory factors exist. Rapid sGC desensitization, in concert with variations in the rate of cGMP breakdown, provides a fundamental mechanism for shaping cellular cGMP responses and is likely to be important in decoding NO signals under physiological and pathological conditions.

Nitric oxide (NO) performs numerous physiological functions, including relaxation of smooth muscle, inhibition of platelet aggregation, and neural communication in the brain (1, 2). A major receptor for NO is the enzyme, soluble guanylyl cyclase (sGC), which catalyzes the production of the effector molecule, cGMP from GTP (3, 4).

Compared with neurotransmitter receptors or related adenylyl and guanylyl cyclases (5, 6), the NO receptor enzyme appears rather unremarkable. It is composed of two different subunits (α and β), but only two isoforms have been shown to exist at the protein level: the $\alpha 1\beta 1$ isoform, which is expressed widely, and the $\alpha 2\beta 1$ isoform present in human placenta (7–9). Also, sGC appears to lack the functional complexity exhibited by related enzymes or receptors. For example, there is no established mechanism for regulation of the enzyme (e.g., by phosphorylation) and, on activation by NO, purified sGC generates cGMP at a constant rate for long periods of time (10, 11). Furthermore, the two naturally occurring sGC isoforms possess very similar functional and pharmacological properties (9).

How sGC responds to NO in living cells, however, has not been investigated, nor is it understood why different cells display very different patterns of NO-stimulated cGMP accumulation ranging from a transient spike-like response (12) to a more slowly developing plateau (13). Here we have analyzed the kinetics of NO-stimulated sGC activity in intact cells. The results show that, in its natural environment, sGC performs differently from what had been assumed from previous biochemical studies. In par-

ticular, within seconds (or less), the enzyme undergoes substantial desensitization. In concert with cGMP-metabolizing enzymes, sGC desensitization enables diverse patterns of cGMP responses to NO to be generated by different cells.

Materials and Methods

Cell Preparations. Cerebellar cells from 8-day-old postnatal rats were prepared and incubated as before (14) except that hydroxyurea pretreatment, used to deplete dividing cells, was used in the initial experiments only (Fig. 2 *a–d*), and the incubation medium contained 100 μ M nitroarginine (to prevent endogenous NO formation) but not BSA. The cells, incubated at 20×10^6 cells/ml, were exposed to the NO donor, diethylamine NONOate (DEA/NO). Decomposed DEA/NO (10 μ M), on its own or in the presence of 1 μ M DEA/NO, did not influence cGMP accumulation. Washed human platelets were prepared and incubated as described (15). When used, phosphodiesterase (PDE) inhibitors were added 10 min before DEA/NO. cGMP was quantified by radioimmunoassay and protein by the bicinchoninic acid method. Extracellular cGMP was measured after filtering the suspensions through 0.6- μ m (cerebellar cells) or 0.22- μ m (platelets) cut-off filters. As found before (13, 14), the amount of cGMP in the medium from cerebellar cells stimulated with DEA/NO was negligible (1–2% of total). Values for extracellular cGMP in the platelet suspensions are given in the main text and Fig. 6 legend. NO concentrations were measured by using an electrochemical probe (World Precision Instruments, Stevenage, Herts, U.K.; Iso-NO electrode). Data are given as means \pm SEM ($n = 3–6$).

sGC Activity in Lysed Cerebellar Cells. Cells were lysed in 10 mM Tris/1 mM DTT (pH 7.4) to give the equivalent of 20×10^6 cells/ml, and sGC activity was assayed in the presence of 1 μ M DEA/NO as before (16) except that Mg^{2+} replaced Mn^{2+} as cofactor, and PDE activity was inhibited by 1 mM EGTA and 1 μ M sildenafil. Under these conditions, a cGMP concentration (2 μ M) similar to that ordinarily produced after 2-min stimulation with DEA/NO was stable over 5 min (i.e., PDE activity was zero).

Immunocytochemistry. Cerebellar cells exposed to DEA/NO (1 μ M) were fixed (4% paraformaldehyde in 0.1 M phosphate buffer) for 30 min at room temperature, resuspended in buffer,

Abbreviations: DEA/NO, diethylamine NONOate; Hb, hemoglobin; NO, nitric oxide; ODO, 1-*H*-[1,2,4]oxadiazolo[4,3-*a*]quinoxalin-1-one; PDE, phosphodiesterase; sGC, soluble guanylyl cyclase.

[†]Present address: Statistical Sciences, SmithKline Beecham, New Frontiers Science Park North, Third Avenue, Harlow, Essex CM19 5AW, United Kingdom.

[§]To whom reprint requests should be addressed. E-mail: john.garthwaite@ucl.ac.uk.

The publication costs of this article were defrayed in part by page charge payment. This article must therefore be hereby marked "advertisement" in accordance with 18 U.S.C. §1734 solely to indicate this fact.

dried onto gelatin-coated slides, rehydrated with distilled water, and permeabilized with 1% Triton X-100 in Tris-buffered saline for 15 min. After rinsing (0.1% Triton X-100/0.2% BSA in Tris-buffered saline), the slides were incubated with normal rabbit and horse sera for 30 min and then with the primary antibodies, sheep anti-cGMP (1:8,000, a gift from J. de Vente, University of Maastricht, the Netherlands) and mouse antigliab fibrillary acidic protein (1:800, Chemicon) overnight at 4°C. After rinsing and incubation with secondary antibodies (anti-mouse FITC and anti-sheep TRITC) for 1 h at room temperature, the slides were mounted and viewed under differential interference contrast and fluorescence optics.

Determination of v_d and v_s . The decline in cGMP levels occurring after deactivation of sGC in cerebellar cells and platelets was fitted to the integrated Michaelis–Menten equation:

$$V_p t = K_p \ln(P_o/P_t) + (P_o - P_t),$$

where P_o = starting cGMP level, P_t = cGMP level at time t , and V_p and K_p are the apparent Michaelis–Menten constants (V_{max} and K_m); V_p , K_p , and P_o were found by iteration (17). The rate of degradation, $v_d = (V_p P)/(K_p + P)$.

The time courses of cGMP accumulation in cerebellar cells and platelets treated with PDE inhibitors were described by a generalized hyperbola.

$$P = (at^n)/(k^n + t^n),$$

where P = cGMP level, a = maximum cGMP level, k is a constant defining the steepness of the hyperbola, and n is a second constant required to give a gradient of zero at $t = 0$, thereby accommodating the brief lag because of mixing and NO dissociation from the donor. Differentiating and inserting the result into the expression, $dP/dt = v_s - v_d$, gives:

$$\frac{ank^n t^{n-1}}{(k^n + t^n)^2} = v_s - \frac{V_p a t^n / (k^n + t^n)}{K_p + a t^n / (k^n + t^n)},$$

from which v_s was found with respect to t .

Results

cGMP Accumulation in Cerebellar Cells. In the first instance, cell suspensions from the postnatal rat cerebellum were used because this brain region has low PDE activity (18), and the dispersed cell preparation eliminates the diffusional constraints inherent in tissue slices (19). DEA/NO, which dissociates with a half-life of 2.1 min, was used as the source of NO. Consistent with previous observations (13), DEA/NO caused large increases in cGMP levels. Although a mixture of cell types is present, heterogeneity of target cell cGMP responses to NO is unlikely to create complications because immunocytochemistry indicated that the increase in cGMP was localized to a discrete subpopulation of cells, the astrocytes. This applied whether the exposure to DEA/NO was 2 min (Fig. 1 *a–c*) or 10 s (not illustrated) and agrees with results obtained from cerebellar slices from rats of the same age (14, 20).

The maximal effect occurred at 0.3 μ M DEA/NO and the EC₅₀ was about 0.1 μ M (Fig. 2*a*). The NO concentration produced in the cell suspension by 0.1 μ M DEA/NO was below the detection limit of an electrochemical probe, indicating that it was less than 20 nM.

Kinetic Analysis of cGMP Formation and Degradation. The rate of cGMP accumulation is simply the difference between its rate of formation by sGC (v_s) and its rate of degradation (v_d) by PDEs

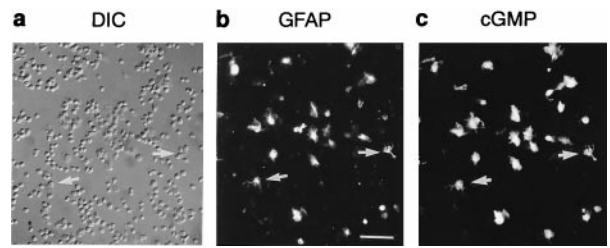


Fig. 1. Location of NO-stimulated cGMP accumulation in cerebellar cell suspension. The same field is shown under differential interference contrast optics (*a*) and after immunofluorescent staining for glial fibrillary acidic protein (*b*) and cGMP (*c*). The cells were fixed after 2-min exposure to DEA/NO (1 μ M). Arrows indicate examples of colocalized staining in individual cells. Bar = 50 μ m.

(or another route). If the rate of cGMP accumulation and v_d are measured, v_s can be determined.

To find v_d , DEA/NO was added to the cells at a supramaximal concentration (1 μ M) to prevent decay of NO being limiting and cGMP accumulation allowed to proceed. Then sGC activity was arrested and the fall in cGMP levels followed with time. Arrest

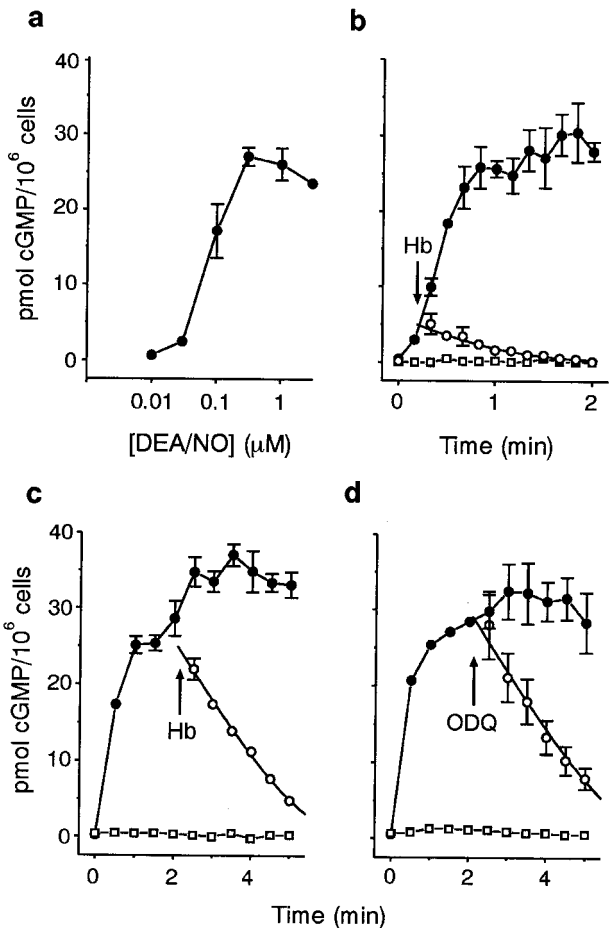


Fig. 2. Characteristics of NO-stimulated cGMP accumulation in cerebellar cells. The concentration–cGMP response curve for DEA/NO (*a*) was obtained by using a 2-min exposure. Deactivation of sGC was determined by addition of Hb (50 μ M) 15 s (*b*) or 125 s (*c*) after DEA/NO (1 μ M) or by addition of ODQ (10 μ M, *d*). ●, controls; □, Hb or ODQ added 5 s before DEA/NO; ○, Hb or ODQ added at arrows; solid lines fit the decline in cGMP to the Michaelis–Menten equation by using identical parameters (K_p and V_p).

of sGC was achieved in two ways. The first was by trapping free NO with hemoglobin (Hb) (21) at a concentration (10–50 μM) that, if added 5 s beforehand, abolished the cGMP response to DEA/NO (Fig. 2 *b* and *c*). Whether added after 15-s (Fig. 2*b*) or 125-s (Fig. 2*c*) exposure to DEA/NO, Hb caused an abrupt cessation of cGMP accumulation and, thereafter, cGMP levels declined progressively. The rate of decline followed Michaelis–Menten-type kinetics, so that v_d could be described operationally by the expression: $v_d = V_p P / (K_p + P)$. Significantly, the parameters K_p and V_p determined by adding Hb after 125 s also described the rate of degradation at lower starting cGMP levels (Hb added at 15 s), indicating that PDE behaves in a simple substrate-linked fashion.

To check the validity of the use of Hb, we tested another strategy: inhibition of sGC with 1-*H*-[1,2,4]oxadiazolo[4,3-*a*]quinoxalin-1-one (ODQ) (22). The results were the same (Fig. 2*d*); moreover, the parameters determined by using the Hb method also described the decay after addition of ODQ, showing that the Hb method for determining v_d is reliable.

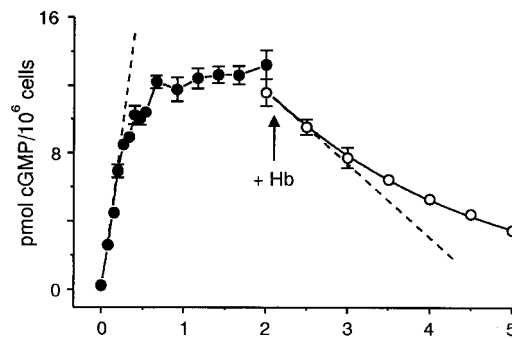
Detailed time courses of the DEA/NO-stimulated accumulation of cGMP showed a steep rate of rise over the initial 15 s that tailed off, giving a quasi-plateau after about 30 s (Fig. 3*a*). At the plateau, by definition, the rate of cGMP degradation equals the rate of cGMP synthesis. The initial rate of cGMP degradation during the plateau was about 0.07 pmol/10⁶ cells/s, implying that sGC was generating cGMP at the same rate. Inspection of the initial rising phase of the cGMP response, however, suggested a rate about 7-fold faster (Fig. 3*a*), pointing to a large decline in enzyme activity with time. The decline could not be attributed to depletion of NO, because the NO concentration was well sustained over 2 min ($0.22 \pm 0.03 \mu\text{M}$; $n = 4$) and because a second dose of DEA/NO (1 μM) added after 2 min did not alter cGMP levels (data not shown).

To extract the kinetics of sGC quantitatively and more accurately, the accumulation of cGMP with time was fitted by a generalized hyperbola (Fig. 3*b*). Differentiation of this expression and correcting for v_d gives v_s , the rate of cGMP synthesis (see *Materials and Methods*). Analysis of the data in this way confirmed that v_s in the intact cells varied dramatically with time after addition of DEA/NO (Fig. 3*b*). Initially, it increased sharply to reach a mean peak of 0.95 ± 0.11 pmol/10⁶ cells/s after 3.8 ± 0.8 s and thereafter declined rapidly to an 8-fold lower rate (0.12 ± 0.08 pmol/10⁶ cells/s) at 2 min ($n = 6$).

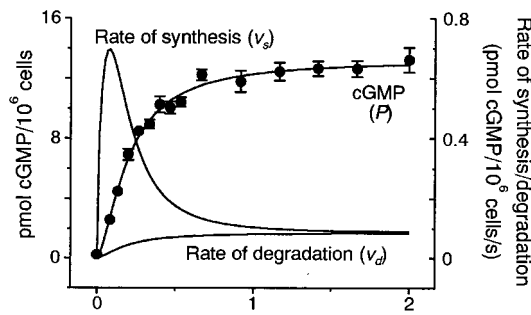
In contrast to this pattern of sGC activity in intact cells, when the enzyme was assayed in lysed cells, the NO-stimulated activity was linear with time (3.5 pmol/10⁶ cells/s; Fig. 3*c*). To test the validity of the analysis of sGC activity in intact cells, therefore, and to check the possible influence of substrate depletion and/or end-product inhibition on the kinetics of sGC, the two determinants of cGMP accumulation, v_s and v_d , were deliberately altered.

Effect of Varying sGC Activity. To reduce v_s , ODQ was used at a concentration (0.3 μM) causing a 70% reduction in the maximum cellular cGMP response to DEA/NO. Under these conditions, the shape of the response was unchanged (Fig. 4*a*). The parameters governing cGMP degradation (K_p and V_p) were also the same (results not shown), indicating a lack of effect of ODQ on PDE activity. Accordingly, the derived kinetic profile of v_s showed exactly the same increase and decrease seen in control cells, despite a peak activity that was 65% lower (Fig. 4*b*). To increase v_s , we used the allosteric sGC activator, YC-1 (23). In the presence of YC-1 (100 μM), the cGMP response to DEA/NO was 3-fold higher than in control cells, but the time courses, again, were similar (Fig. 4*a*). Because YC-1 stabilizes the binding of NO to sGC (24) and can inhibit PDE activity (25), v_d could not be determined. Therefore, v_s was derived for the extreme cases of PDE activity being normal (using the v_d found

a Intact cells: cGMP levels



b Intact cells: kinetic analysis



c Lysed cells

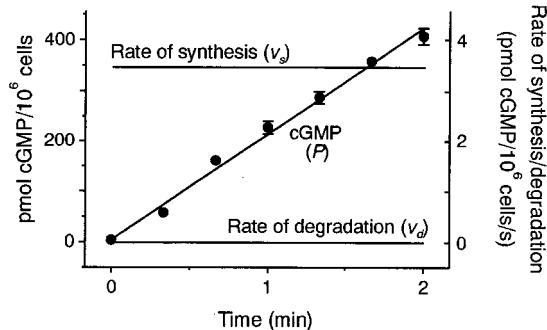


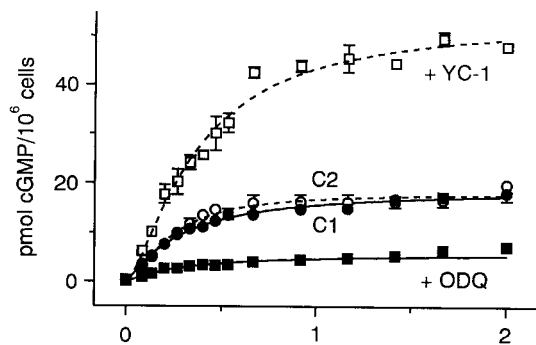
Fig. 3. Kinetics of cGMP synthesis and degradation in intact (*a* and *b*) and lysed (*c*) cerebellar cells. Filled symbols (*a*–*c*) represent cGMP levels after addition of DEA/NO (1 μM). Open symbols (*a*) chart the decline in cGMP after addition of Hb (at arrow); the data are fitted to the Michaelis–Menten equation (solid line). Broken lines (*a*) indicate the differing initial rates of cGMP accumulation and degradation. In *b*, the progress curve for cGMP accumulation (data from *a*) is fitted by a generalized hyperbola and v_d and v_s determined as described in *Materials and Methods*. In lysed cells (*c*), the linear cGMP accumulation is equivalent to an sGC activity of 4,140 pmol/mg protein/min; v_d was eliminated by PDE inhibition.

in control cells) and zero. In both cases, v_s increased to a peak rate double that of control cells and then decreased (Fig. 3*b*).

Thus, over a wide range of sGC activity resulting in a 10-fold variation in the accumulation of cGMP, the amplitude of v_s changed in a predictable way, but its kinetic profile stayed the same.

Effect of Reducing PDE Activity. The aim was to eliminate v_d and so determine v_s directly from the experimental data. An effective way of inhibiting cGMP breakdown in the cerebellar cells was with a combination of sildenafil and rolipram. In the presence of

a cGMP accumulation



b Rates of synthesis (v_s)

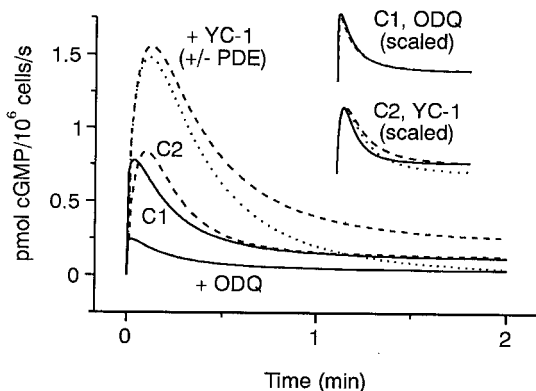


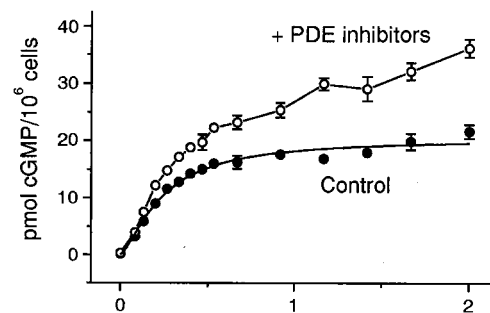
Fig. 4. Pharmacological manipulation of v_s in cerebellar cells. In *a*, addition of $0.3 \mu\text{M}$ ODQ (■) decreased cGMP relative to the control (C1, ●); $100 \mu\text{M}$ YC-1 (□) increased cGMP relative to the control (C2, ○). In all cases, the cells were stimulated with $1 \mu\text{M}$ DEA/NO and the time courses were fitted by a generalized hyperbola. The derived profiles of v_s from these data are shown in *b*. For YC-1-treated cells, profiles assuming control PDE activity (dashed line) and zero PDE activity (dotted line) are both shown. In *insets*, the profiles of v_s are scaled by peak height; solid lines are the controls.

these PDE inhibitors, the cGMP response progressively exceeded that of control cells (Fig. 5*a*). Because cGMP degradation was negligible over the relevant time intervals (Fig. 5*b*), v_d can be taken as zero. Differentiation of the cGMP response then gives v_s . The profile of v_s obtained in this way superimposed accurately on the profile determined by using the usual method (Fig. 5*c*).

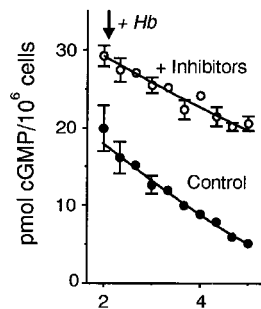
Recovery from Desensitization. This was studied by first stimulating the cells with DEA/NO ($1 \mu\text{M}$) for 2 min to induce desensitization. Then, Hb ($10 \mu\text{M}$) was added and, after various intervals, DEA/NO was reapplied at a concentration ($100 \mu\text{M}$) sufficient to overcome the effect of Hb. Analysis of the mean initial rate of rise in cGMP levels indicated that sGC was able to recover fully from desensitization within 10 min, the half-time being about 1.5 min (results not shown).

Kinetics of cGMP in Platelets. To investigate whether sGC desensitization might be a general property of the enzyme, experiments were conducted by using human platelets. Consistent with a previous study (26), addition of DEA/NO ($1 \mu\text{M}$) led to a transient increase in cGMP, peaking after 15 s and then falling to a much lower steady state (Fig. 6*a* and *c*). Under control conditions, cGMP breakdown in platelets was too fast to be

a



b



c

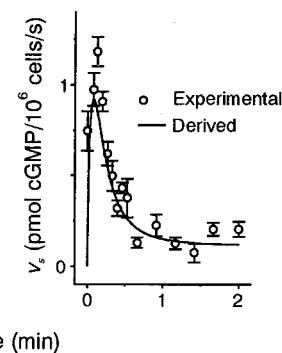


Fig. 5. Effect of PDE inhibition in cerebellar cells. In *a*, addition of PDE inhibitors ($100 \mu\text{M}$ sildenafil + $1 \mu\text{M}$ rolipram) (○) increased the cGMP response to DEA/NO ($1 \mu\text{M}$) relative to control (●). The control response was fitted by the usual hyperbolic function (solid line). In *b*, decay of cGMP levels is shown after addition of $10 \mu\text{M}$ Hb in the presence (○) and absence (●) of the PDE inhibitors. Solid lines fit the data to the Michaelis–Menten equation. In *c* are the profiles of v_s generated by differentiating the cGMP data obtained in the presence of the PDE inhibitors (○) and by the usual analysis of the control cGMP accumulation data (solid line). Differentiation was carried out by using MICROCAL ORIGIN software, Ver. 4.10.

measured. A combination of the PDE inhibitors, sildenafil and erythro-9-(2-hydroxy-3-nonyl)adenine greatly reduced the rate of cGMP degradation such that it was similar to the uninhibited rate observed in cerebellar cells (Fig. 6*a* *Inset*). Under these conditions, the platelet cGMP response was transformed from a small brief transient into one that was 10-fold larger and that had a hyperbolic shape resembling that found normally in cerebellar cells (Fig. 6*a*). Accordingly, deconvolution indicated that v_s rose sharply and then fell, much as in cerebellar cells (Fig. 6*b*).

A prediction is that if v_d is increased (i.e., inhibition is removed), the transient cGMP response normally observed in platelets in the absence of PDE inhibitors should be regained. PDE catalytic efficiency, as determined in the presence of the inhibitors, was augmented by increasing V_p or by decreasing K_p . In both cases, a transient cGMP response similar to the measured one was obtained (Fig. 6*c*), the main difference being that an increased V_p (47-fold) apparently matched better the later falling and steady-state phases. The latter phase of the measured response is artifactual, however, because the cGMP in the platelet suspension after 2 min appeared to be all extracellular (equivalent to $24.0 \pm 1.2 \text{ pmol cGMP/mg protein}$). The simulation obtained by decreasing K_p (210-fold) should be more applicable, because it corresponds to removal of competitive inhibition (27), and it appeared to be so because it undershot the later phases.

Discussion

Analysis of NO-stimulated sGC activity in intact cells has revealed several properties that were unexpected from the

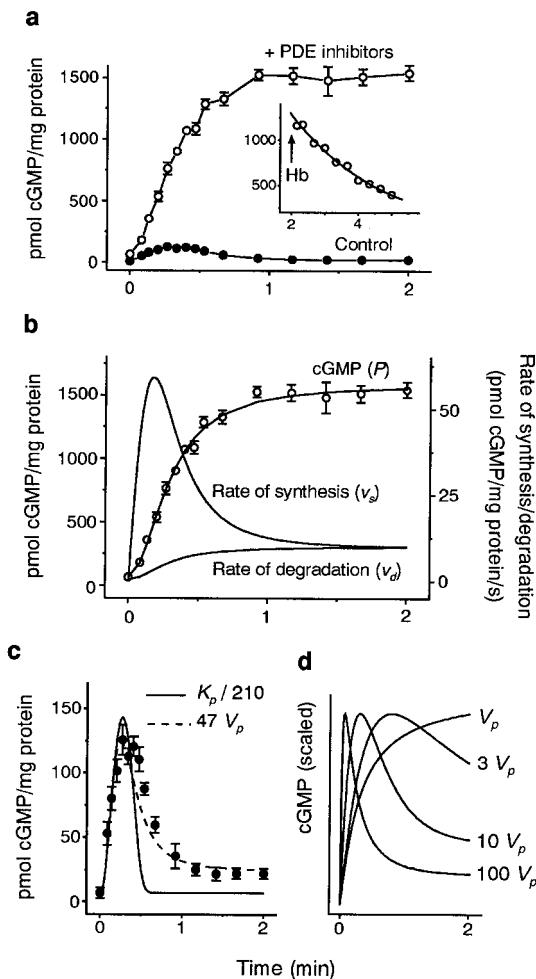


Fig. 6. Kinetics of cGMP synthesis and degradation in human platelets. The accumulation of cGMP induced by DEA/NO ($1 \mu\text{M}$) in the presence (\circ) and absence (\bullet) of PDE inhibitors ($100 \mu\text{M}$ sildenafil + $100 \mu\text{M}$ erythro-9-(2-hydroxy-3-nonyl)adenine) is in *a*. (*Inset*) Decay of cGMP levels after addition of $10 \mu\text{M}$ Hb in the presence of the PDE inhibitors, fitted by the Michaelis-Menten equation. At the 2-min time-point, extracellular cGMP accounted for 52 ± 8 pmol/mg protein (about 3% of total), which was subtracted from each data point. The analysis of v_s and v_d in the presence of the PDE inhibitors is shown in *b*, together with the raw data. In *c*, the cGMP response in control platelets (\bullet) is shown; the parameters, V_p and K_p , describing cGMP breakdown in the presence of the PDE inhibitors were altered by increasing V_p or decreasing K_p as indicated. In *d* are depicted the different shapes of cGMP response (scaled to the peaks) that would be produced by a combination of a desensitizing v_s and increases in V_p (both derived from cerebellar cells stimulated with DEA/NO). Reductions in K_p have broadly similar effects, except that with a low K_p , the late phase becomes truncated (cf. solid line in *c*).

behavior of the enzyme in tissue homogenates or in its purified form.

First, the potency of NO in cells is greater than has been reported for purified sGC (the $\alpha 1\beta 1$ isoform), where an EC_{50} of 250 nM was estimated (28). However, other studies that used DEA/NO found an EC_{50} of about 100 nM (29), suggesting a greater potency, though the resulting NO concentration was not measured directly. In the cerebellar cells, which we have found to express $\alpha 1$ and $\beta 1$ mRNA and protein (B. Gibb & J.G., unpublished observations), NO is at least an order of magnitude more potent. This finding, which is consistent with the potency of NO to relax vascular smooth muscle ($\text{EC}_{50} = 10$ nM) (30), helps define the physiologically relevant range of NO concentrations and suggests that current thinking about the distance

over which an NO source exerts biological effects (31) will need revision.

Second, an important determinant of the dynamics of NO-sGC signaling is the rate at which sGC deactivates. Measurements of the off-rate of NO from purified sGC, assuming this represents the deactivation rate, have yielded confusing results. When Hb or myoglobin was used to trap NO, the half-life of the NO-sGC complex was estimated to be about 2 min at 37°C (32, 33). From a physiological perspective, this is very slow and difficult to reconcile with the rate at which smooth muscle recovers from NO-induced relaxation (34). A later investigation concluded that, with GTP and Mg^{2+} present, the half-life fell to about 5 s (35), but a different study claimed a 3-min half-life under these conditions (32). A particularly relevant experiment was when Hb was added during the early steeply rising phase of cGMP accumulation in the cerebellar cells (Fig. 2*b*). Just 5 s later, cGMP was not only significantly less than in control cells but was at the level predicted should the amount of cGMP at this time be governed solely by PDE activity (i.e., residual sGC activity was zero). Other experiments in which Hb was added later gave concordant results. Hence, in living cells, sGC deactivation occurs with a half-life of no more than a few seconds and possibly much less, allowing sGC to respond dynamically to fluctuations in NO concentration.

The third and most surprising result was that NO-stimulated sGC activity, both in rat cerebellar cells and in human platelets, underwent rapid desensitization. This phenomenon is unlikely to be peculiar to exogenously added NO, because the kinetics of cGMP accumulation observed in the cerebellar cells in the present study is very similar to those occurring in the same cells when endogenous NO production is provoked (13, 14, 19). Consistent with the type of desensitization we describe also existing *in vivo* is the finding that the hypotensive effects of nitrovasodilators are enhanced when endogenous NO formation is inhibited acutely, an effect attributed from *in vitro* experiments, to reflect alterations in the sensitivity of smooth muscle sGC to NO (36).

Desensitization appeared to curtail sGC activity within a few seconds of addition of the NO source but because these very early kinetics will also be influenced by the rate of dissociation of NO from the donor, desensitization may well set in earlier. Recovery from desensitization, by comparison, was slow, taking several minutes to be complete. Fast entry into and slow exit from the desensitized state are characteristics classically associated with neurotransmitter receptors (37). The kinetics of onset and recovery clearly distinguishes sGC desensitization recorded in our experiments from sGC down-regulation (sometimes also called "desensitization") typically seen after chronic (hours-days) exposure to NO-releasing agents and which probably reflects destabilization of subunit mRNA and/or protein (38-40).

The mechanism of sGC desensitization remains unknown. Depletion of substrate (GTP) or direct end-product inhibition (by cGMP) appear not to participate because the desensitization kinetics was little changed despite variations of 6-fold in sGC activity and 10-fold in cGMP levels. That sGC failed to desensitize when assayed in lysed cerebellar cells agrees with numerous previous studies (10, 11, 16) and suggests the existence of a cellular factor that loses its activity (possibly by dilution) in cell-free preparations. Because sGC activity in the lysed cells was about 4-fold higher than the peak activity recorded in intact cells (Fig. 3*b* and *c*), the endogenous factor could function as an inhibitor. A previous study has suggested that there is a protein inhibitor of sGC in bovine lung (41), although it remains to be characterized. Recently, Ca^{2+} was found to inhibit sGC (42), but only at concentrations orders of magnitude higher than those normally found free in the cytosol. Accordingly, sGC desensitization in cerebellar cells was unaffected by removal of extra-

cellular Ca²⁺ or by intracellular loading with Ca²⁺ chelators (unpublished observations), suggesting that Ca²⁺ is not involved.

Functionally, desensitization of sGC works in concert with PDE activity to shape the cellular cGMP response to NO. That is, as PDE activity differs (43), sGC desensitization imposes varying patterns of cGMP accumulation, ranging from a brief low-amplitude transient (with high PDE activity) to a large sustained plateau (with low PDE activity) or a mixture of the two (Fig. 6d). This range of behavior encompasses all the shapes of cGMP response to NO that we have encountered in the literature. The varying temporal and amplitude characteristics are expected to be important in the differential selection of downstream transduction pathways [e.g., high-affinity cGMP-dependent protein kinases vs. low affinity cGMP-gated ion channels (44)].

In conclusion, NO-stimulated sGC activity within a cellular environment is more complex than previously assumed, implying the existence of hitherto unknown regulatory factors. The rapid on- and off-kinetics and the desensitizing profile of activity indicate that the properties of sGC are much more akin to those of a neurotransmitter receptor than previous evidence had suggested. The possibility that alterations in sGC regulation contribute to clinical conditions associated with abnormal tissue responsiveness to NO, such as vascular disorders (45) and erectile dysfunction (46), merits investigation.

This work was supported by The Wellcome Trust and a Medical Research Council (U.K.) Studentship (to T.C.B.). Our thanks to Dr. M. P. Gorge for expert help with platelet experiments and to Dr. J. de Vente (University of Maastricht, the Netherlands) for the kind gift of cGMP antiserum.

1. Moncada, S., Palmer, R. M. & Higgs, E. A. (1991) *Pharmacol. Rev.* **43**, 109–142.
2. Garthwaite, J. & Boulton, C. L. (1995) *Annu. Rev. Physiol.* **57**, 683–706.
3. Waldman, S. A. & Murad, F. (1987) *Pharmacol. Rev.* **39**, 163–196.
4. Ignarro, L. J. (1991) *Biochem. Pharmacol.* **41**, 485–490.
5. Sunahara, R. K., Dessauer, C. W. & Gilman, A. G. (1996) *Annu. Rev. Pharmacol. Toxicol.* **36**, 461–480.
6. Drewett, J. G. & Garbers, D. L. (1994) *Endocr. Rev.* **15**, 135–162.
7. Hobbs, A. J. (1997) *Trends Pharmacol. Sci.* **18**, 484–491.
8. Denninger, J. W. & Marletta, M. A. (1999) *Biochim. Biophys. Acta* **1411**, 334–350.
9. Russwurm, M., Behrends, S., Harteneck, C. & Koesling, D. (1998) *Biochem. J.* **335**, 125–130.
10. Katsuki, S., Arnold, W., Mittal, C. & Murad, F. (1977) *J. Cyclic. Nucleotide Res.* **3**, 23–35.
11. Gerzer, R., Hofmann, F. & Schultz, G. (1981) *Eur. J. Biochem.* **116**, 479–486.
12. Saito, M. & Deguchi, T. (1979) *Biochim. Biophys. Acta* **586**, 473–480.
13. Garthwaite, J., Charles, S. L. & Chess Williams, R. (1988) *Nature (London)* **336**, 385–388.
14. Garthwaite, J. & Garthwaite, G. (1987) *J. Neurochem.* **48**, 29–39.
15. Gorge, M. P., Meyer, D. J., Hothersall, J., Neild, G. H., Payne, N. N. & Noronha Dutra, A. (1995) *Br. J. Pharmacol.* **114**, 1083–1089.
16. Bunn, S. J., Garthwaite, J. & Wilkin, G. P. (1986) *Neurochem. Int.* **8**, 179–185.
17. Fernley, H. N. (1974) *Eur. J. Biochem.* **43**, 377–378.
18. Greenberg, L. H., Troyer, E., Ferrendelli, J. A. & Weiss, B. (1978) *Neuropharmacology* **17**, 737–745.
19. Garthwaite, J. (1985) *Br. J. Pharmacol.* **85**, 297–307.
20. de Vente, J., Bol, J. G. J. M., Berkelmans, H. S., Schipper, J. & Steinbusch, H. M. W. (1990) *Eur. J. Neurosci.* **2**, 845–862.
21. Gibson, Q. H. & Roughton, F. J. W. (1957) *J. Physiol. (London)* **136**, 507–526.
22. Garthwaite, J., Southam, E., Boulton, C. L., Nielsen, E. B., Schmidt, K. & Mayer, B. (1995) *Mol. Pharmacol.* **48**, 184–188.
23. Koesling, D. (1998) *N. Schm. Arch. Pharmacol.* **358**, 123–126.
24. Friebe, A. & Koesling, D. (1998) *Mol. Pharmacol.* **53**, 123–127.
25. Friebe, A., Mullershausen, F., Smolenski, A., Walter, U., Schultz, G. & Koesling, D. (1998) *Mol. Pharmacol.* **54**, 962–967.
26. Salvemini, D., Radziszewski, W., Korbut, R. & Vane, J. (1990) *Br. J. Pharmacol.* **101**, 991–995.
27. Corbin, J. D. & Francis, S. H. (1999) *J. Biol. Chem.* **274**, 13729–13732.
28. Stone, J. R. & Marletta, M. A. (1996) *Biochemistry* **35**, 1093–1099.
29. Schrammel, A., Behrends, S., Schmidt, K., Koesling, D. & Mayer, B. (1996) *Mol. Pharmacol.* **50**, 1–5.
30. Carter, T. D., Bettache, N. & Ogden, D. (1997) *Br. J. Pharmacol.* **122**, 971–973.
31. Vaughn, M. W., Kuo, L. & Liao, J. C. (1998) *Am. J. Physiol.* **274**, H1705–H1714.
32. Brandish, P. E., Buechler, W. & Marletta, M. A. (1998) *Biochemistry* **37**, 16898–16907.
33. Kharitonov, V. G., Sharma, V. S., Magde, D. & Koesling, D. (1997) *Biochemistry* **36**, 6814–6818.
34. Palmer, R. M., Ferrige, A. G. & Moncada, S. (1987) *Nature (London)* **327**, 524–526.
35. Kharitonov, V. G., Russwurm, M., Magde, D., Sharma, V. S. & Koesling, D. (1997) *Biochem. Biophys. Res. Commun.* **239**, 284–286.
36. Moncada, S., Rees, D. D., Schulz, R. & Palmer, R. M. (1991) *Proc. Natl. Acad. Sci. USA* **88**, 2166–2170.
37. Jones, M. V. & Westbrook, G. L. (1996) *Trends Neurosci.* **19**, 96–101.
38. Filippov, G., Bloch, D. B. & Bloch, K. D. (1997) *J. Clin. Invest.* **100**, 942–948.
39. Waldman, S. A., Rapoport, R. M., Ginsburg, R. & Murad, F. (1986) *Biochem. Pharmacol.* **35**, 3525–3531.
40. Ujji, K., Hogarth, L., Danziger, R., Drewett, J. G., Yuen, P. S., Pang, I. H. & Star, R. A. (1994) *J. Pharmacol. Exp. Ther.* **270**, 761–767.
41. Kim, T. D. & Burstyn, J. N. (1994) *J. Biol. Chem.* **269**, 15540–15545.
42. Parkinson, S. J., Jovanovic, A., Jovanovic, S., Wagner, F., Terzic, A. & Waldman, S. A. (1999) *Biochemistry* **38**, 6441–6448.
43. Beavo, J. A. (1995) *Physiol. Rev.* **75**, 725–748.
44. Kramer, R. H. & Karpen, J. W. (1998) *Nature (London)* **395**, 710–713.
45. Katz, S. D., Schwarz, M., Yuen, J. & LeJemtel, T. H. (1993) *Circulation* **88**, 55–61.
46. Christ, G. J., Kim, D. C., Taub, H. C., Gondre, C. M. & Melman, A. (1995) *Can. J. Physiol. Pharmacol.* **73**, 1714–1726.